A MULTI-SCALE NUMERICAL METHODOLOGY FOR PREDICTING THE MECHANICAL PROPERTIES OF POROUS CFRP LAMINATES USING DATA FROM X-RAY COMPUTERIZED TOMOGRAPHY

Konstaninos I. Tserpes and Antonios G. Stamopoulos

Laboratory of Technology & Strength of Materials, Department of Mechanical Engineering & Aeronautics, University of Patras, Patras, 26500, Greece

Keywords: CFRP laminates, X-ray CT, Porosity, Progressive Damage Modeling, Finite element analysis

Abstract

In the present work, proposed is a multi-scale finite element model for predicting the mechanical properties of porous CFRP laminates by exploiting data from the novel and promising X-ray Computerized Tomography technique. The model integrates three analysis levels; namely the analysis of a representative unit cell (RUC) containing the small pores, the analysis of the RUC containing the large pores clustered in a single pore using the novel MObject (Mean Object) approach and the simulation of the CFRP specimen. The porosity characteristics (volume fraction, shape, volume, location) were evaluated from the CT scans using the VGStudio MAX software. The software parameters are validated using optical microscopy. At the RUCs and the specimen, progressive damage modeling is applied to predict the homogenized properties of the porous matrix, which are transferred to the next level, and the mechanical properties of the specimen, respectively.The model was applied in the case of transverse tension of unidirectional laminates under three porosity levels and the numerical results (transverse stiffness, transverse tensile strength) were compared with results from mechanical tests obtaining a good agreement. Both methods show a small reduction in transverse stiffness, which increases with increasing porosity volume fraction and a considerable decrease in tensile strength.

1. Introduction

Despite the implementation of advanced manufacturing techniques, porosity in the matrix of carbon fibre reinforced plastics is introduced mostly during the manufacturing process [1-3]. As a form of initial defect it has a severe impact in the mechanical performance of the composite structures especially in the matrix dominated mechanical properties as seen in previous research [4-8]. Considering the previously mentioned effect of porosity, it's detection is crucial. Among the non destructive techniques existing, the X-ray computerized tomography appears as the most promising method for the detection of pores as ti combines high accuracy, 3-dimensional view and detailed information about the porosity characteristics. To this end, a significant number of research has been conducted aiming to explore the method's capabilities [9] in characterizing the material [8, 10-11], in situ measurments in mechanical tests [12-13] or even improve the method in terms of accuracy, data manipulation and corresponding equipment [14-15]. Despite that progress, the development of numerical tools capable of utilizing data about defect characteristics obtained by X-ray CT scans in order to predict the residual properties of composite parts was limited. It is worth mentioning the research of Drach et al. [16] where x-ray CT scans were used to create finite element models aiming to calculate the elastic properties of the matrix of and Straumit et al. [17] where computerized

tomography was utilized for the creation of voxel model considering the fibre misalignment as initial defect.

In the present work, a numerical metholodoly is presented which takes as input the porosity characteristics derived from X-ray CT scans' analysis to predict the mechanical properties of CFRP laminates by implementing the progressive damage modeling (PDM) in different simulation levels.

2. Methodology

The proposed methodology starts from the CT image analysis and the defect detection where all the pores and voids were quantified. The CT image analysis was validated with optical microscopy. Having a large ratio between the voids and the small pores in terms of pore size, the multi-level analysis was implemented which divided the methodology in three levels, namely the small pores level, the large voids level and the specimen's level. In the first two levels only the epoxy resin of the CFRP was considered. The output of the lower level was the input of the next higher level. The mechanical behavior of the epoxy resin was previously obtained by mechanical tests of the neat resin. The proposed methodology was implemented for the case of the transverse tensile test. In parallel, actual mechanical tests were conducted in specimens made from porous CFRP plates from samples of which the CT data was obtained. The flowchart of the proposed methodology can be seen in Fig.1
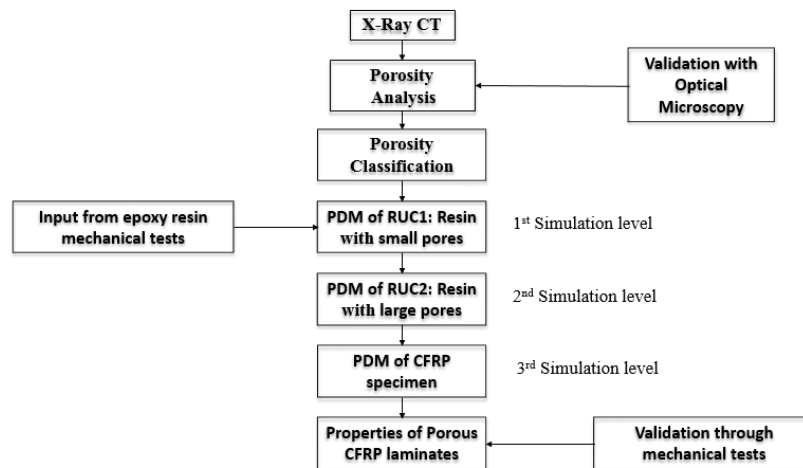

Figure 1. The flowchart of the proposed multi-level methodology

3. Experimental

3.1 Mechanical tests of the epoxy resin

Aiming to obtain the mechanical behavior of the epoxy resin, mechanical tests were conducted, namely tension, compression and shear tests. The epoxy resin used was the EhKF420C, the same resin used for the manufacturing of the CFRP plates. The corresponding standard followed was the ASTM D638 [18] with the use of Tinius Olsen universal testing machine with 5kN capacity for the tensile tests, ASTM D695 [19] with the MTS servohydraulic machine with 100kN capacity for the compression and ASTM E143 [20] along with the Hydropuls Schenck of 250kN capacity for the torsion tests respectively. 5 specimens were used for each test. The obtained mechanical behavior can be seen in Fig.2.

3.2 Transverse tensile test

The transverse tensile test was conducted in specimens of 3 different porosity content achieved by implementing different pressure in the autoclave as seen in [9] namely minimum, medium and

Konstantinos I Tserpes and Antonios G Stamopoulos

extensive porosity. The specimens were made of 16 plies of the EhkF420 epoxy resin and 24k carbon fibres in direction perpendicular to the loading axis.The ASTM D3039 [21] standards were followed and the MTS servohydraulic universal testing machine with 100kN capacity was used. 5 specimens of each category were tested.
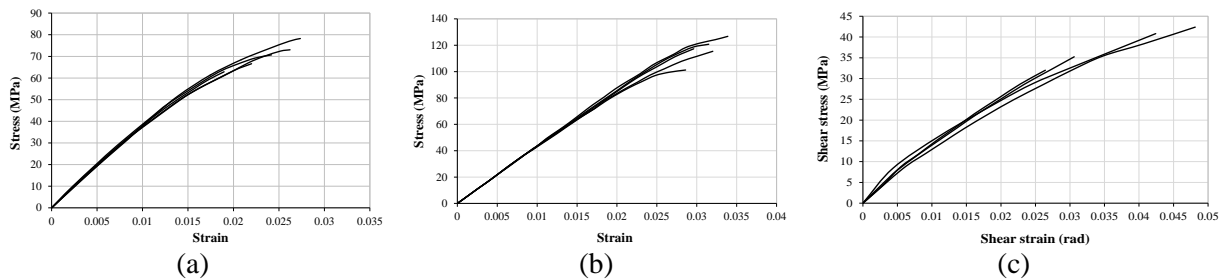
(a)   (b)   (c)

Figure 2. Obtained tensile (a), compressive (b) and torsional curves (c)

4. Porosity Detection and Classification

The X-ray CT method was implemented in samples cut from the CFRP plates from which the tensile specimens were cut. The resolution and the CT parameters were briefly described in [9]. The CT data obtained was analysed with the use of VG Studio MAX software by implementing the standard automatic global threshold and the least possible minimum detectable size. The porosity volume fraction was found to be 1.56% for the case of minimum porosity, 1.62% for the case of the medium porosity and 3.43% for the case of the extensive porosity samples. In parallel, the sample with the most intense porosity was inspected with a Leica DM/LM optical microscope and a Leica DFC295 recorder. Three different planes were inspected 0.5, 1 and 1.5 mm depth measured from the outer surface of the sample. As the large pores were easily located, the interest was concentrated in the areas around them. The obtained images revealed a large number of small pores, a part of which was bellow the resolution limitation of the CT scans. A typical example of the comparison between the CT scan measurement and the optical microscopy and the smaller pores can be seen in Fig.3.
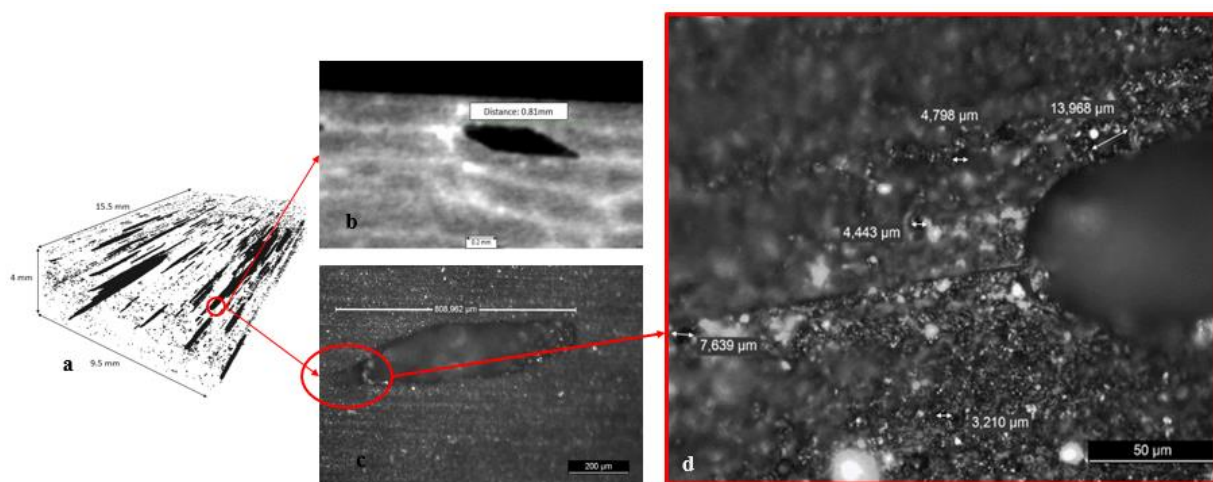
Figure 3. A set of pores as detected by the VG Studio MAX software (a), a large pore as measured in the VG Studio MAX (b) via optical microscopy (c) and the small pores formatted around the edge of it (d) as seen in the oprical microscope

Having a significant difference and ratio between the small pores' and the large pores' size, the implementation of multi-level analysis [22] was chosen. To this end, the detected porosity was divided

Konstantinos I Tserpes and Antonios G Stamopoulos

into two major categories, namely small pores (dimension less than 1mm) which was used in the 1st simulation level and the large pores which was used for the 2nd simulation level. The small pores were subdivided into 3 major categories: from almost 0 to 0.2 mm, 0.2+ to 0.6 mm and 0.6+ to 0.99 mm maximum dimension. By calculating the average dimension of each subcategory, selecting the minimum amount of pores of the 3rd subcategory and keeping the contribution of each subcategory to the volume fraction of the small pores constant, equivalent sets of pores were extracted.

5. Progressive Damage Modeling

The progressive damage modeling was used in all the simulation levels aiming to calculate the mechanical behavior and properties with the presense of the detected porosity. The geometries' creation and the simulations were performed with the use of ANSYS FE code [23].

5.1 RUC1-1st Simulation Level

As previously mentioned, the small pores were taken into account. For each porosity level a cubic representative unit cell (RUC) was created which contained the sets of pores as previously extracted. The pores in this level are spherical, randomly distributed and not overlapped (agglomerated). The dimensions of the RUC are controlled by the porosity volume fraction. The geometry of the RUC1s can be seen in Fig.4.
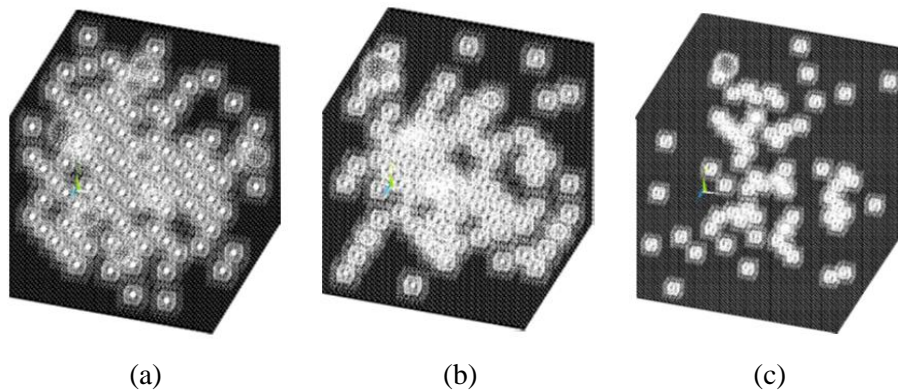

(a)   (b)   (c)

Figure 4. The developed Representative Unit Cells for the 1st simulation level for the Minimum (a), Medium (b) and Extensive porosity (c) samples

A multilinear isotropic hardening was used to describe the material behavior.The Progressive Damage Modeling was implemented with the use of the Christensen failure criterion [24] for isotropic ductile materials as seen in the following equation.

$$\left(\frac{1}{S_T} - \frac{1}{S_C}\right)(\sigma_x + \sigma_y + \sigma_z) + \frac{1}{S_T S_C}\left\{\frac{1}{2}\left[(\sigma_x - \sigma_y)^2 + (\sigma_y - \sigma_z)^2 + (\sigma_x - \sigma_z)^2\right] + 3(\sigma_{xy}^2 + \sigma_{yz}^2 + \sigma_{xz}^2)\right\} \quad (1)$$
$$-1 \leq r$$

Where S_T, S_C the tensile and compressive strength of the material as given from the mechanical tests. The developed models were subjected to tension, compression and planar shear load. The parameter r was used for the implemented material degradation, a concept introduced by Matzenmiller et al. [25]. According to it:

$$E = (1 - \bar{\omega})E_0 \quad and \quad G = (1 - \bar{\omega})G_0 \quad (2)$$

$$where \quad \bar{\omega} = 1 - e^{\frac{1}{m}(1 - r^m)} \quad (3)$$

Konstantinos I Tserpes and Antonios G Stamopoulos

For the previously mentioned FE models, a parametric study was conducted for the determination of the damage parameter m (m value was considered equal to 1) and the mesh density.

5.2 RUC2-2nd Simulation Level

For the second simulation level and the three porosity levels, Representative Unit Cells (RUC2) were created that contained not all the large pores but an equivalent mean pore (Mean Object-MObject) as seen in [26]. The MObjects of the three scanned samples can be seen in Fig.5.
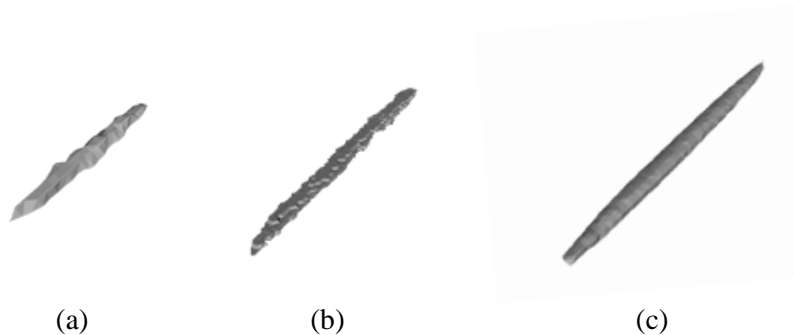

(a)   (b)   (c)

Figure 5. The MObjects of the Minimum (a) , Medium (b) and Extensive porosity (c) samples

The large pores by this technique were clustered and an equivalent pore with respect to the size and shape was created. Then with the use of ANSYS Workbench and ANSYS APDL was placed in the center of an RUC dimensioned relatively to the average pore size and analogicaly to the large pores' volume fraction. The meshed RUC2 of the Extensive porosity level can be seen in Fig.6.
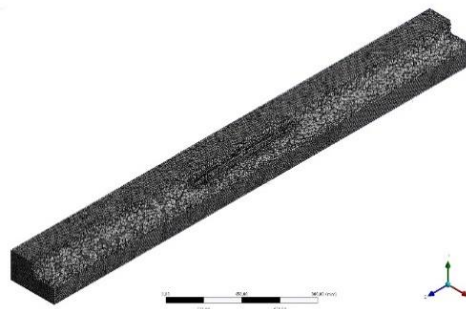

Figure 6. The meshed Representative Unit Cell of the 2nd simulation level with the MObject placed in the center

The material behavior obtained from the previous level was used as input to the current as the elements were considered to have isotropic material properties. The Christensen failure criterion was also implemented as well as the material softening behavior, just like in the previous level. The model was subjected to tensile, compressive and shear deformation in all directions, and the results in terms of stiffness and strength showed no significant dependency to the loading axis considering that the volume fraction of the MObject is less than 3% and the RUC2 dimensions are analogicaly formatted to the average diamensions of the MObject.

5.3 CFRP Specimen-3rd Simulation level

In the final simulation level the residual properties of the resin and the properties of the fibres were combined using micromechanical equations so as to calculate the ply properties. For the elastic properties the Chamis equations [27] were used and for the ply strength the micromechanical

equations as described by Daniel et al [28]. The Progressive Damage Model was also used in this level and the Hashin failure criteria [29] were implemented along with a knockdown parameter 0.2 [30] for the properties degradation. The specimen gage section was modeled, therefore the length was 125 mm while the crossectional area was rectangular (2 mm x 25 mm). The obtained behavior of the model compared with the mechanical tests for the three porosity levels can be seen in the following figure.
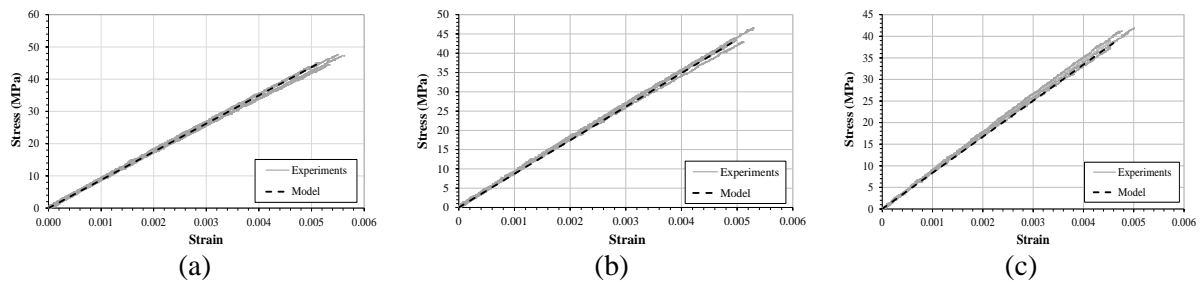

(a)   (b)   (c)

Figure 7. Comparison of the model and the mechanical tests for the three different porosity levels, namely Minimum (a), Medium (b) and Extensive porosity (c).

In Fig.8 the overall results of the stiffness and the strength are presented for all the 3 porosity contents along with the standard deviation observed in the mechanical tests.
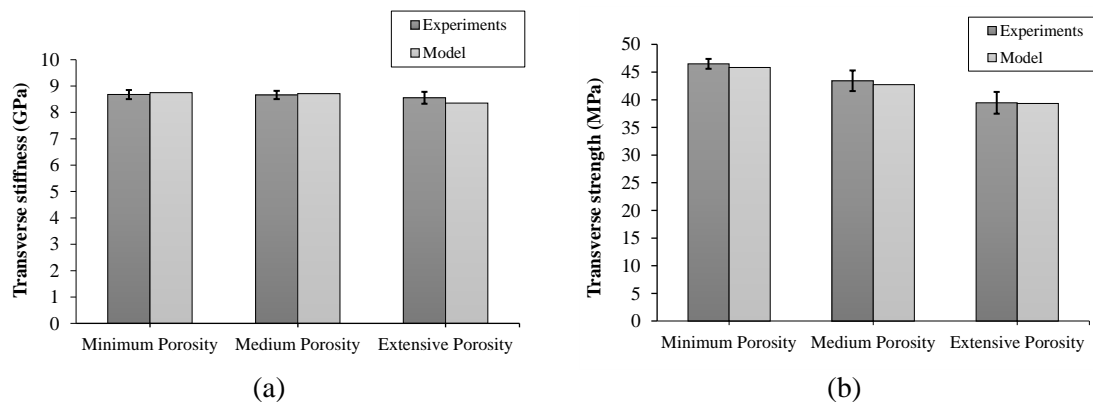

(a)   (b)

Figure 8. (a) Numerical vs. experimental transverse stiffness values and (b) Numerical vs. experimental transverse tensile strength values

6. Conclusions

Herein, a numerical methodology was developed for simulating the mechanical behavior of porous CFRP UD laminates by exploiting data extracted from X-ray CT scans. The link between X-ray CT data and numerical simulation is based on the assumption that the porosity characteristics of the samples scanned apply also to the CFRP specimens modeled. Fundamental for the efficiency of the methodology is the validation of software parameters used for the analysis of porosity. The methodology was applied to simulate the transverse tensile behavior of three different UD CFRP laminates containing pores of different contents. The numerical results correlate very well with experimental results, thus validating the methodology. Based on the above it can be stated that the proposed methodology represents a robust step towards the development of a linkage between the X-ray CT NDT method and numerical simulation and may serve as a basis for the development of large-scale models to be applied in the quality control and structural integrity inspection of composite structural parts.

Konstantinos I Tserpes and Antonios G Stamopoulos

Acknowledgments

References

[1] P. Olivier, J.P. Cottu and B. Ferret. Effects of cure cycle pressure and voids on some mechanical properties of carbon/epoxy laminates. *Composites* 26:509–515, 1995

[2] F.Y.C. Boey and S.W. Lye. Void reduction in autoclave processing of thermoset composites. Part 1: high pressure effects on void reduction. *Composites* 23: 261–265, 1992

[3] Y .Gu, L. Li, Z. Zhang and Z. Sun. Void formation model and measuring method of void formation condition during hot pressing process. *Polymer Composites* 2010

[4] H. Huang and R. Talreja. Effects of void geometry on elastic properties of unidirectional fiber reinforced composites. *Composites Science Technology* 65:1964–1981, 2005

[5] M.R. Wisnom, T. Reynolds and N.Gwilliam. Reduction in interlaminar shear strength by discrete and distributed voids. *Composites Science and Technology* 56: 93–101, 1996

[6] N.L. Costa, S.F.M. Almeida and M.C. Rezende. The influence of porosity on the interlaminar shear strength of carbon/epoxy and carbon/bismaleimide fabric laminates. *Composites Science and Technology* 61: 2101_2108, 2001

[7] S.F.M. Almeida and Z.S. Nogueira-Neto. Effects of void content on the strength of composite laminates. *Composites Structure* 28: 139–148,1994

[8] A.G. Stamopoulos, K.I. Tserpes, P. Prucha and D.Vavrik. Evaluation of the mechanical Evaluation of porosity effects on the mechanical properties of carbon fiber-reinforced plastic unidirectional laminates by X-ray computed tomography and mechanical testing. *Journal of Composite Materials* 2015

[9] M. Krumm,C. Sauerwein, V. Hämmerle and R. Oster. Capabilities and application of specialized Computed Tomography methods for the determination of characteristic material properties of fiber composite components. *Proceedings of the International Conference of Thermoelectrics ICT/ECT Aalborg, Denmark*, July 9-12

[10] Y. Nikishkov, L. Airoldi and A. Makeev. Measurement of voids in composites by X-ray Computed Tomography.*Composites Science Technology* 89: 89–97, 2013

[11] V. Crupi, G. Epasto and E. Gulgielmino. Computed Tomography analysis of damage in composites subjected to impact loading. *Frattura ed Integrità Strutturale* 17: 32-41, 2011

[12] A.E. Scott , M. Mavrogordato, P. Wright, I. Sinclair, S.M. Spearing. In situ In situ fibre fracture measurement in carbon–epoxy laminates using high resolution computed tomography. *Composites Science and Technology* 71:1471-1477, 2011

[13] Y. Nikishkov, G. Seon, A. Makeev and B.Shonkwiler.In-situ measurements of fracture toughness properties in composite laminates. *Materials and Design* 94:303–313, 2016

[14] J. Kastner, B. Plank, D.Salaberger , J. Sekelja. Defect and Porosity Determination of Fibre Reinforced Polymers by X-ray Computed Tomography. *Proceedings of the 2nd International Symposium on NDT in Aerospace* 2010-We.1.A.2.

[15] I. Jandejsek, J. Jakubek, M. Jakubek, P. Prucha, F. Krejci, P. Soukup, D. Turecek, D. Vavrik and J. Zemlicka. X-ray inspection of composite materials for aircraft structures using detectors of Medipix type. *Proceedings of the 15th International Workshop on Radiation Imaging Detectors* 23–27 June, Paris, France 2013

[16] B. Drach, I. Tsukrov, T. Gross, S. Dietrich, K. Weidenmann, R. Piat and T. Bohlke. Numerical modeling of carbon/carbon composites with nanotextured matrix and 3D pores of irregular shapes. *International Journal of Solids and Structures* 48: 2447-2457, 2011

[17] I. Straumit, S. Lomov, I. Verpoest and M. Wevers. Determination of the local fibers orientation in a composite material from a micro-CT data. *Proceedings of Composites Week Leuven and TEXCOMP-11 Conference*, 16-20 September, Leuven, Belgium, 2013

[18] Standard Test Method for Tensile Properties of Plastics. Designation: D638-01. American Society for Testing of Materials (ASTM).

[19] Standard Test Method for Compressive Properties of Rigid Plastics. Designation: D695-02a. American Society for Testing of Materials (ASTM).

[20] Standard Test Method for Shear Modulus at room temperature. Designation: E143-02. American Society for Testing of Materials (ASTM).

[21] Standard Test Method for Tensile Properties of Polymer Matrix Composites. Designation: D3039-D3039M-95a. American Society for Testing of Materials (ASTM).

[22] G. Ernst, M. Vogler, C. Hühne and R. Rolfes. Multiscale progressive failure analysis of textile composites. *Composites Science and Technology* 70: 61–72, 2010

[23] ANSYS User's manual, Version 11 (2008). Swanson Analysis Systems, Pittsburgh, PA, USA

[24] R.M. Christensen. A two property yield failure (fracture) criterion for homogeneous, isotropic materials. *Journal of Engineering Materials and Science* 126:45, 2004

[25] A. Matzenmiller, J. Lublinear, R.L. Taylor. A constitutive model for anisotropic damage in fiber-composites. *Mechanics of Materials* 20: 125–152, 1995

[26] C. Heinzl, J.Weissenbock, A.Reh, J.Kastner, T.Dierig, T.Gunther, D.Kiefel and R.Stossel. Software tools for robust extraction, analysis and visualization of porosities in XCT scans of fiber-reinforced polymers. *In Proceedings of the 6th International Symposium on NDT in Aerospace*, 12-14 November, Madrid, Spain, 2014

[27] C.C Chamis. Mechanics of composite materials: Past, Present and Future. NASA Technical Memorandum 100793. *21st Annual Meeting of the Society for Engineering Science*, Blacksburg, Virginia, October 15-17, 1984.

[28] I.M Daniel, O. Ishai. *Engineering Mechanics of Composite Materials*. Oxford University Press 1994. ISBN 0-19-507506-4

[29] Z. Hashin.Failure criteria for unidirectional fiber composites. *Journal of Applied Mechanics* 47(2):329-334, 1982.

[30] S.C. Tan, *Stress Concentrations in Laminated Composites*. Technomic Publishing Company 1994. ISBN 1-56676-077-1